Talanta 99 (2012) 586–593

Contents lists available at SciVerse ScienceDirect

Talanta

journal homepage: www.elsevier.com/locate/talanta

Separation and analysis of lanthanides by isotachophoresis coupled with inductively coupled plasma mass spectrometry

Laurent Vio [a,c,*], Gérard Crétier [c], Frédéric Chartier [b], Valérie Geertsen [d], Alkiviadis Gourgiotis [a], Hélène Isnard [a], Jean-Louis Rocca [c]

[a] Commissariat à l'Energie Atomique, Saclay, DEN/DPC/SEARS/LANIE, 91191 Gif sur Yvette Cedex, France
[b] Commissariat à l'Energie Atomique, Saclay, DEN/DPC, 91191 Gif sur Yvette Cedex, France
[c] Université de Lyon, Institut des Sciences Analytiques (UMR CNRS 5280), Villeurbanne, France
[d] Commissariat à l'Energie Atomique, Saclay, DSM/IRAMIS/SIS2M/LIONS, 91191 Gif sur Yvette Cedex, France

ARTICLE INFO

Article history:
Received 6 February 2012
Received in revised form
7 June 2012
Accepted 15 June 2012
Available online 20 June 2012

Keywords:
Isotachophoresis
Inductively coupled plasma mass spectrometry
Coupled techniques
Lanthanides
Fission products
Nuclear industry

ABSTRACT

This study is a large project initiated by the French Nuclear Agency, and concerns the development of a new electrolyte system for the separation of lanthanides by isotachophoresis. This new system is based on a leading electrolyte that incorporates 2-hydroxy-2-methylbutyric acid as complexing agent. The optimization of separation conditions (complexing agent concentration, pH, capillary dimensions, injection conditions, and current intensity) performed by experiments on a commercial capillary instrument with contactless conductivity detection, which allows to improve the separation of 13 lanthanides (La to Lu, except Pm and Ho). We have also directly coupled the isotachophoresis to an inductively coupled plasma mass spectrometer to visualize the mono-elementary elution bands and demonstrate the potentiality of the method for isotope ratio measurements. The application to a simulated solution representative of a fraction of fission products present in a MOX spent fuel is presented in this paper to demonstrate the possible application in future on nuclear fuel samples.

1. Introduction

In the nuclear industry, the knowledge of isotope composition and elemental concentration of actinides (U, Pu, Am, and Cm) and fission products (lanthanides, Cs, etc) is crucial for qualification of neutronic calculation codes [1], burn-up determination [2] and management of nuclear waste. Fission product solutions, particularly lanthanides are characterized by mass spectrometry techniques i.e. thermal ionization mass spectrometry (TIMS) [3] (TIMS) or multiple-collector inductively coupled plasma mass spectrometry (MC ICP–MS) [4], in order to obtain precision and accuracy on isotope ratio of a few ‰. The direct determination of lanthanide isotope composition by mass spectrometry is hampered by isobaric interferences as well as oxide formation. High resolution mass spectrometers cannot resolve these interferences and so previous chemical separations are then required before mass spectrometric analysis.

This work initiated by the CEA Saclay is a part of a large project concerning the development of a new analytical system for the isotopic characterization of lanthanides in nuclear fuel samples. This system must be in accordance with the As Low As Reasonably Achievable principle (ALARA [5]), and the goal is to decrease the total effective dose equivalent and the radioactive liquid waste volume during the chemical separation steps.

For the determination of lanthanide isotope composition in nuclear fuel samples two strategies are applied. In the first one, the elements of interest are individually collected by performing successive chemical separations and analyzed by TIMS or MC ICP–MS (ICP–QMS). In this off-line procedure, lanthanides (fission products) are separated by ion exchange chromatography (IEC) [3,4,6]. In the second strategy, IEC is directly coupled to quadrupole ICP-MS [7–11] (ICP–QMS) or MC ICP-MS [12]. This on-line method simplifies the sample preparation procedure and then decreases the handling time of radioactive materials. However, hyphenation of IEC with ICP-MS is not in response to the need of decreasing radioactive liquid waste volume. Capillary electrophoresis (CE) is very attractive in the nuclear field because it offers minimal waste generation, high separation efficiency, low cost and fast analysis. So, in order to reduce both the sample amount and the effluent volume, hyphenation of capillary electrophoresis (CE) with ICP-MS was developed [13–15]. In this case, the sample injection volume decreases by a factor three without loss of resolution. Nevertheless, due to the insufficient sensitivity,

* Corresponding author at: Commissariat à l'Energie Atomique, Saclay, DEN/DPC/SEARS/LANIE, 91191 Gif sur Yvette Cedex, France.
E-mail address: laurent.vio@gmail.com (L. Vio).

0039-9140/$ - see front matter © 2012 Elsevier B.V. All rights reserved.
http://dx.doi.org/10.1016/j.talanta.2012.06.041

preconcentration processes are usually required [16]. Unlike other CE techniques, isotachophoresis (ITP) separation itself leadsto a self-sharpening effect at the zone boundaries and preconcentration capability all along the analysis [17]. The use of ITP as both preconcentration and the separation method provides high stacking effect and separation if the electrolyte system is properly adjusted. ITP is a basic mode of CE using discontinuous electrolyte systems, i.e. leading electrolyte (LE) and terminating electrolyte (TE). The first one governs the migration speed, separation capability and sample preconcentration whereas the second one which has the lowest electrophoretic mobilities in the system closes the electric circuit. After separation of the zones of analytes according to their effective mobility, a pseudo-stationary state is reached where all the adjacent bands of analytes are migrating with a constant speed. In ITP, each element is eluded as a quasi-rectangular band and at a concentration fixed by separate conditions, independent from the element concentration in the sample.

The work presented here deals with the development of the isotachophoretic separation of lanthanides for applications in nuclear fuel samples. The separation of lanthanides is a very old and difficult task due to their similarities in their physical and chemical properties [18]. Whatever the separation techniques used, a significant enhancement of the selectivity between lanthanides can be achieved by the addition of complex-forming agents. The most effective agent is 2-hydroxyisobutyric acid (HIBA) which is frequently reported for the separation of lanthanides by IEC [3,12,19–23], CE [24–27] and ITP [28–29]. Among the other complexing agents tested, 2-hydroxy-2-methylbutyric acid (HMBA) was shown to exhibit higher efficiency for the IEC separation of lighter elements of the lanthanide series [30].

In the first part of this paper, the best composition of leading electrolyte (nature, concentration and pH) and the optimal separation conditions (dimensions of the separation capillary, current intensity, injected amount) are defined from experiments carried out with a commercial capillary equipment using a contactless conductivity detector (ITP–CD). Then, in the second part the separation system interfaced to an inductively coupled plasma quadrupole mass spectrometer (ITP–CD–ICP–QMS) is evaluated for the lanthanides of interest from a simulated spent MOX fuel solution.

2. Materials and methods

2.1. Chemicals and samples

All solutions were prepared with purified water provided by a Purelab UHQ II system (Elga, Le Plessis Robinson, France). For the preparation of electrolyte solutions and the coating of capillaries, chemicals (HIBA (99%), HMBA (98%), sodium acetate (99.99%), ammonia solution (25%), acetic acid (100%), sodium chloride (99.5%), sodium hydroxide (30%), hydrochloric acid (37%) and polyvinyl alcohol (PVA, 89,000–98,000 Da, 99+% hydrolyzed)) were obtained from Sigma Aldrich (Isle d'Abeau, France).

Standard solutions of elements obtained from Spex Certiprep Group (Longjumeau, France) were at the concentration of 1000 or 10,000 mg L^{-1} in 5% nitric acid. In order to prepare stock solutions of each lanthanide at a concentration of 1000 mg L^{-1} without nitrates, aliquots of stock solutions were evaporated to dryness at 90 °C and dry extracts were dissolved in adequate volumes of pure water. These individual stock solutions were used to prepare four different sample solutions containing 13 lanthanides (La to Lu, except Pm and Ho), 7 lanthanides (La, Pr, Sm, Gd, Dy, Tm and Lu), 6 lanthanides (Ce, Nd, Eu, Tb, Er and Yb) and a mixture of the 4 lanthanides of great interest in nuclear industry (Nd, Sm, Eu and Gd). Thiourea was added to the mixture of 7 and 6 lanthanides. The simulated sample of spent MOX fuel solution containing 24 elements is prepared from natural standard using the same protocol as lanthanide samples. Its chemical composition is given in Table 1. For all experiments, the free nitrate standards are diluted to a leading electrolyte according to the conditions of the study.

Table 1
Chemical composition of the fission product fraction of a simulated spent MOX fuel after U and Pu extraction.

Element	Concentration (ng/μL)
Se	0.45
Rb	2.73
Sr	6.33
Y	3.54
Zr	29.55
Mo	29.16
Ru	21.51
Rh	3.21
Pd	15.75
Ag	0.69
Cd	1.23
Sn	0.72
Sb	0.18
Cs	21.03
Ba	15.30
La	10.26
Ce	20.46
Pr	9.45
Nd	34.80
Sm	6.42
Eu	1.53
Gd	2.04
Tb	0.03
Dy	0.03

2.2. Preparation of coated capillaries

In some experiments, the separation capillary was coated with PVA prior to use in order to reduce electro-osmotic flow (EOF) and consequent dispersion phenomena. An acidic solution of 5% PVA (pH 1 with HCl) in water is prepared and degassed using sonication. After connection to a pressure vessel (Nanobaume capillary packing unit, Western Fluids Engineering, Wildomar, CA, USA), the capillary is successively rinsed with NaOH 1 mol/L and HCl 1 mol/L by applying 2 bar for 30 min in each rinsing step. Then, the capillary is emptied with N_2 at 2 bar for 10 min. The capillary coating is performed flowing the PVA solution through the capillary for 90 min at 5 bar. Finally, the capillary is placed in a gas chromatography oven (GC 17, Shimadzu, Kyoto, Japan) and heated at 145 °C for 8 h under 2 bar continuous N_2 flow.

2.3. Isotachophoretic separations

Isotachophoretic separations were performed using a HP3D electrophoresis system (Agilent Technologies, Waldbronn, Germany) and a Tracedec contactless conductivity detector (Innovative Sensor Technologies, Vienna, Austria). The silica capillaries (360 μm o.d.) are provided by Cluzeau Info Labo (Sainte Foy La Grande, France).

Different capillary configurations were used. In mono-capillary configuration, the capillary has an inner diameter of 30 or 75 μm and the separation length L_S is defined as the capillary length that is not filled by sample after injection. In coupled capillary configuration, a 150 μm i.d. × 8 cm length injection capillary (corresponding to a volume of 1.4 μL) is connected to a separation capillary (30 μm i.d.) without dead volume by means of a 350 μm

i.d. × 1/16 o.d. × 1 cm length PTFE tubing. In the latter case, L_S is equal to the length of separation capillary. Whatever the capillary configuration maybe, the L_S value is specified for each experiment.

Before separation, a first experiment is performed to set the injection step. With the conductivity detector placed at 16 cm from the capillary inlet (effective volume = 0.11, 0.71 and 1.47 μL for 30 μm i.d. mono-capillary configuration, 75 μm i.d. mono-capillary configuration and coupled capillaries configuration, respectively), the capillary is washed under 1 bar pressure for 30 min with leading electrolyte. Then, a small amount of pure water is injected into the capillary and flushed with leading electrolyte under 40 mbar. The corresponding flow rate is calculated from the water migration time. For separation, the conductivity detector is placed at 14 cm from the capillary outlet. Before each run, the capillary is flushed with the leading electrolyte under 1 bar for 1 min. Then, sample is hydrodynamically injected by pressurizing the solution under 40 mbar during an injection time calculated from the set injection volume and the previously determined flow rate. For storage, the capillary is cleaned with pure water and flushed with N_2 under 2 bar for 1 h.

2.4. Calculation of isotachophoretic resolution

In isotachophoresis, when the steady state is reached, analytes in the sample zone are organized in adjacent mono-elementary bands with diffused boundary regions (Fig. 1A). Isotachophoretic resolution R_s is defined for a single analyte as the ratio of the separated amount Q_P to the injected amount Q_i [31]. The separated amount Q_P is represented by the plateau duration t_P. The injected amount Q_i corresponds to the band width t_B measured in time at half-height. So, R_s is written as

$$R_S = Q_P/Q_i = t_P/t_B \quad (1)$$

The signal recorded with the conductivity detector is composed of steps separated by diffuse boundary regions (Fig. 1B). To estimate t_B and t_P, the detection signal is derived and the diffused boundary regions appear as Gaussian peaks (Fig. 1C). t_B corresponds to the time between the peak tops. According to the Normal distribution, t_P is given by

$$t_P = t_B - 3\sigma_1 - 3\sigma_2 \quad (2)$$

where σ_1 and σ_2 are the standard deviations of peaks. Taking into account Eqs. (1) and (2), R_s is calculated by

$$R_S = 1 - (3\sigma_1 + 3\sigma_2)/t_B \quad (3)$$

Data analysis (calculation of the derived signal, t_B, σ_1, σ_2, t_P and R_S) is performed using the software Origin 8.1 provided by OriginLab Corporation (Northampton, Massachusetts, USA).

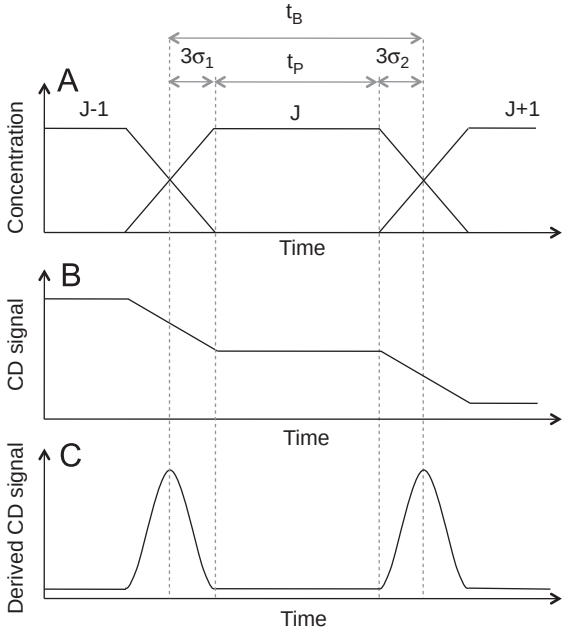

Fig. 1. Visualization of the parameters used to calculate isotachophoretic resolution of solute j from conductimetric signal. t_B = band width. t_P = plateau duration. σ_1 and σ_2 = standard deviations of the peaks observed from the derived CD signal.

2.5. Determination of lanthanide effective mobilities

For isotachophoretic lanthanide separation, the complexing agent added to the leading electrolyte (HIBA or HMBA) is a weak organic acid (noted HA) that undergoes a dissociation/protonation equilibrium:

$$HA \leftrightarrow H^+ + A^- \quad (4)$$

The complexing ligand (A^-) migrates against the lanthanide ion (Ln^{3+}) which then forms various complexes according to the following equation:

$$Ln^{3+} + pA^- \leftrightarrow LnA_p^{(3-p)+} \quad (5)$$

Thus, various species of the lanthanide ion (Ln^{3+}, LnA^{2+}, LnA_2^+ and LnA_3) are present and their distributions are dependent on the nature of the complexing agent, their total concentrations and the pH of the leading electrolyte. Consequently, these three parameters also govern the lanthanide ion' effective mobility μ_j that is equal to the weighted average of the mobilities of the individual species.

The determination of the effective mobilities of lanthanides for different compositions of the leading electrolyte was performed by CE, on a 75 μm i.d. × 360 μm o.d. × 60 cm length silica capillary, using the leading electrolyte as a separation electrolyte. In order to avoid co-elution between two successive elements in the lanthanide series, the 13 lanthanides of interest were injected in two different batches. The first one containing thiourea, La, Pr, Sm, Gd, Dy, Tm and Lu, the second one containing thiourea, Ce, Nd, Eu, Tb, Er and Yb. Thiourea was used to measure electroosmotic flow. The lanthanide effective mobility μ_j was calculated by the classical equation:

$$\mu_j = (L\ l/U)(1/t_j - 1/t_0) \quad (6)$$

where L is the total length of the capillary, l is the effective separation length (between the capillary inlet and the detection cell), U is the applied voltage (the runs were driven at 25 kV), t_j is the migration time of lanthanide j and t_0 is the migration time of thiourea.

2.6. Determination of critical selectivity

In electromigration methods, selectivity α_j between two neighboring analytes j and $j+1$ (where $j+1$ has the lowest mobility) is expressed as the relative difference in their effective electrophoretic mobilities [32]:

$$\alpha_j = \left(\mu_j - \mu_{j+1}\right)/\mu_{j+1}. \quad (7)$$

When the sample mixture is composed of more than two analytes, selectivity is calculated for each pair of neighboring analytes and the critical selectivity α_{min} is defined as the minimum of all calculated selectivities. This quantity was shown to directly condition the maximum attainable resolution in ITP [33] and can be used to compare the separation possibilities of different electrolyte systems.

Table 2
Instrument settings of the ICP–QMS.

Parameter	Value/ description
Make-up flow	10 μL/min
RF power	1100 W
Nebulizer gas flow	0.7–0.8 L/min
Auxiliary gas flow	0.9 L/min
Cool gas flow	15 L/min
Peak width (10%)	0.82 amu
Scan mode	Peak jumping
Dwell time	50 ms

2.7. ICP—QMS detection

2.7.1. Spectrometer settings

The spectrometer used is an ICP–QMS X series^{II} Thermo Electron. Optimization of the experimental parameters was carried out without electrophoretic separation, with a Nd test solution in order to obtain the maximum counting rates on $^{142}Nd^{+}$. Settings like torch position, gas flows and ion focusing were daily optimized. The general operating conditions are summarized in Table 2. After signal optimization, signal stability and oxides formation were controlled by calculating the relative standard deviation (RSD) for ten consecutive integrations and by measuring the $^{142}NdO^{+}/^{142}Nd^{+}$ isotope ratio. The RSD varied between 2% and 4% and oxides typical values were less than 2%.

2.7.2. Interface

The Mira Mist CE (Burgener Research, Mississauga, Ontario, Canada) interface was used for the ITP and ICP–QMS hyphenation. The parallel flux nebulizer used in this interface is able to operate with low sample flow rates (3–10 μL/min) without suction effects that could degrade the separation [34]. The separation capillary is passed through a T-piece and is positioned directly inside the nebulizer. The optimal capillary position was found by controlling the ICP–MS sensitivity for a given element in different capillary positions. The optimum capillary position is inside the nebulizer at about 1 mm from the nebulizer nozzle. The cathodic electrical connection is achieved by means of an additional make-up flow (10 μL/min) of leading electrolyte directly introduced into the nebulizer by a syringe pump (Harvard Apparatus, Holliston, MA, USA).

The nebulizer is connected to a linear PTFE micro-spray chamber (Burgener Research). For sample flows between 10 and 15 μL/min, according to the manufacturer, this chamber provides a high efficiency transport of the sample to the torch.

3. Results and discussion

3.1. Design of the electrolyte system via CE separation

For the electrolyte design, we have chosen in this study to respect the "C, H, O, N principle", that is widely applied in the nuclear field for easy laboratory liquid waste elimination reasons. More precisely, this principle consists of using only reagents made of carbon, hydrogen, oxygen or nitrogen atoms, which results in forming only non-corrosive compounds during waste elimination process [35]. This principle has to be applied not only to the complexing agent but also to any compound in the leading and terminating electrolytes or in the interface make-up flow. The hyphenation imposes also the development of an electrolyte system that fits ICP–MS analysis conditions. So, the use of high concentrations of inorganic salts (such as sodium ion) and organic compounds in separation process has to be avoided to prevent ICP-MS cones blocking and matrix effects.

Prior performing any ITP separation of lanthanides, it was necessary to choose the best complexing agent. HIBA and HMBA show the same bite distance formed by two oxygen atoms from an OH and a COOH group and only differ from the OH substituted carbon steric hindrance [28]. The lanthanide complex stability constants are available in the literature for various organic acids such as HIBA [36] or HMBA [37]. For each organic acid, the lanthanide complex stability increases with the metal atomic number. This is attributed to the lanthanide' ionic radius contraction occurring along the period. Stability constant comparison shows that HMBA forms less stable complexes than HIBA, probably because of higher alkyl group steric effect for HMBA when compared to HIBA. The stability constant variation along the considered lanthanide period is much larger for HMBA than for HIBA, which should result in higher separation ability. In order to confirm this hypothesis, the dependence of the effective mobility μ_j of lanthanide ions on the complexing agent concentration and electrolyte pH were studied by CE. The electrolyte is a 10 mM acetic acid solution adjusted to the desired pH by the addition of ammonia and the ligand concentration varies in the range 2–25 mM. The pK_a values for HIBA and HMBA are 3.97 and 4.05, respectively. So, the studied pH range is between pH=4 and pH=5.5. For pH values lower than ligand pK_a, complexation is insufficient to involve selectivity. Above pH=5.5, precipitation of hydroxides occurs for the heaviest lanthanides [38]. Whatever maybe the complexing agent, the effective mobility of lanthanides is a decreasing function of the ligand concentration because increasing complexing agent concentration favours the formation of the less charged species such as 1: 2 and 1: 3 metal:ligand complexes. Migration order of lanthanide is independent from both nature and concentration of the complexing agent as governed by stability order. However, the decrease of electrophoretic mobility especially those of the heavier element is more intense with HIBA, which suggests a weaker chelating capacity for HMBA. These results are in agreement with Good's work comparing the stability constant of many complexing agents such as lactic acid and HIBA with lanthanides [34]. Those conclusions have also been suggested by Raut et al. in LC [30], but never applied in ITP.

To simultaneously optimized the separation using all parameters involved i.e nature of the complexing agent, its concentration and pH of the electrolyte, the critical selectivity α_{min} was determined for each tested lead electrolyte conditions. The graphic representation of α_{min} variations versus both lead electrolyte ligand concentration and pH value (Fig. 2). With HIBA as complexing agent (Fig. 2.A), the optimal conditions obtained for [HIBA]=13–17 mM and pH=4.3 to 5.1, which correspond to an α_{min} value between 0.08 and 0.1. With HMBA as ligand (Fig. 2B), the maximal value of α_{min} is obtained for [HMBA]=12.5–18.5 mM at pH=4.4–5.2, which allows to obtain α_{min}=0.1–0.12. At this point of the study, HMBA appears to be the best candidate for the fission product separation since its use under the optimal conditions entails a critical selectivity α_{min} which is 20% larger than HIBA, leading to an easier separation.

3.2. Leading and terminating electrolytes for ITP separation

To demonstrate the validity of our approach, the CE optimal separation conditions are used to formulate the two leading electrolyte compositions and perform the ITP separations of thirteen lanthanides in mono-capillary configuration (Fig. 3). More precisely the ammonium ions introduced in the leading electrolytes for pH adjustment play the part of leading cation. The terminating electrolyte is a 15 mM acetic acid solution. In this case, the migration of the very mobile cation H^{+} is affected by the

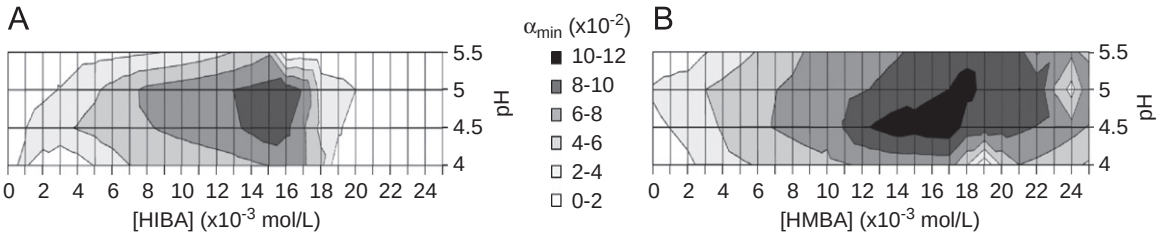

Fig. 2. Dependence of the critical selectivity α_{min} between lanthanides on complexing agent concentration and pH value. Electrolyte: complexing agent + 10 mM acetic acid, pH value adjusted with ammonia. Complexing agent = HIBA (A), HMBA (B).

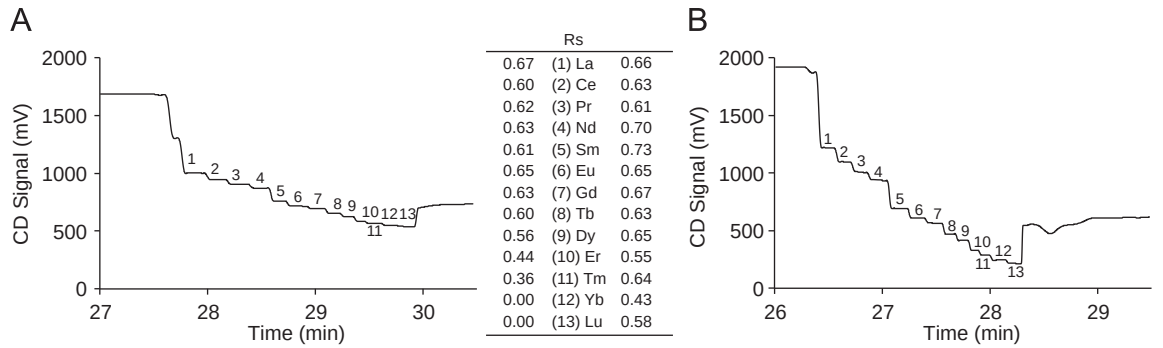

Fig. 3. ITP–CD separation of lanthanides under optimal conditions for each complexing agent. Sample: 13 lanthanide mixture. Injected amount of each solute = 100 ng. Mono-capillary configuration: capillary inner diameter = 75 μm, separation length L_S = 116 cm, injection volume = 1 μL. Leading electrolyte: complexing agent + 10 mM acetic acid, pH value adjusted to 4.5 with ammonia. Complexing agent: 14 mM HIBA (A), 14 mM HMBA (B). Terminating electrolyte: 15 mM acetic acid. Current intensity = 9 μA.

presence of the buffering acetate anion migrating in the opposite direction. Protons recombine with this counter ion according to the dissociation constant of acetic acid. H^+ effective mobility is then controlled by appropriate selection of conditions [39] and hydrogen ion can serve as the terminating cation. In order to rigorously compare the results obtained from HMBA and HIBA, resolution R_S of each elementary band is computed according to the method explained earlier. Experiments in Fig. 3 respect the ITP principle described by Everaerts et al. [17] which indicates that, under the same current density and injection conditions, the separation time depends only on the leading ion mobility. HIBA and HMBA are homologous compounds and their optimal conditions for the lanthanides separation are close. Even if EOF is not suppressed and the ionic strength slightly differs in the two experiments, differences in resolution mostly depend on the complexing agent used. With an average value of 0.63 for each element, the resolutions obtained with HMBA are clearly better than those obtained with HIBA for which the average resolution is about 0.45 (with HIBA, the two last elements, Yb and Lu, are not separated (R_S = 0)).

The acetate concentration has also been studied in both terminating and leading electrolytes (data not shown). From the stability constants of both complexing agents, the contribution of acetic acid as complexation assistant agent can be neglected. However it plays a key role as a buffer agent. In the leading electrolyte, decreasing acetic acid concentration below 10 mM results in losing the separation of light lanthanides. Above 15 mM, acetic acid concentration shows no influence on migration. Acetic acid concentration was thus fixed at 10 mM in the leading electrolyte. In the terminating electrolyte, the concentration of the acetic acid showing no influence on the separation ranging from 5 to 20 mM, its concentration was then fixed at 15 mM. Finally, the optimal electrolyte system for ITP separation of lanthanides is the following one: leading electrolyte = 14 mM HMBA + 10 mM acetic acid, pH adjusted to 4.5 with ammonia and terminating electrolyte = 15 mM acetic acid.

Nuclear spent fuel solutions contain not only lanthanides but also large amounts of actinides as well as various light elements. At the CEA Saclay, analysis of radioactive trivalent elements (lanthanides, Am, Cm) is always performed after matrix (U, Pu) removal. At this point, it is important to study the performance of the separation optimized previously in the presence of residual uranium. U is a stronger Lewis acid than Lu, showing higher stability constant with HIBA than any lanthanide [40]. By analogy between HIBA and HMBA, it can be deduced that, under optimal chelating condition, its electrophoretic mobility may be reduced enough for it to be eluded at the last position that is just before the terminating electrolyte. Consequently, whatever is the composition of purified sample, the leading electrolyte selected would be able to bear residual U contribution. This was verified by comparing the isotachophoregram of the 13 lanthanide mixture to the same mixture spiked with a uranium amount three times higher (data not shown). For different reasons the separation was extended to minor elements such as cesium (Cs) for its interest in nuclear field and yttrium (Y) usually considered as one lanthanide. Lanthanide mixture spiked with Cs and Y at the same concentration as that of lanthanides was separated (data not shown). It appears that whatever is its complexation behavior with HMBA, Cs shows no interferences with lanthanides. Cs has a higher mobility than lanthanides and forms a plateau between the leading electrolyte and the first lanthanide La. However, already pointed out by Hirokawa et al. [41] the separation of Y from lanthanides (mixt with Dy) remains an issue which should involve a future adjustment of the leading electrolyte composition. However, the isotopic ratio measurements of both Y and Dy should not be affected because these elements do not share any isotopes. Two more elements (Am, Cm) must be taken into account when dealing with spent fuel solutions. Americium and

curium hydrated ionic radius are included between those of neodymium and samarium [42]. Their migration order can then easily be predicted as situated between Nd and Sm. This prediction is in agreement with the results obtained by Perna et al. [43] in IEC in the presence of HIBA where Am and Cm show retentions that are intermediate between Nd and Sm. From the studies of lanthanide electrophoretic mobilities for both ligands it can be concluded that the mobility difference between Nd and Sm is wider for HMBA than HIBA. The higher selectivity provided by HMBA would permit the insertion of two more plateaus.

3.3. Optimization of separation conditions for hyphenation

This part describes the approach setup to satisfy isotope ratio measurements, that are large plateaus (t_P), small diffusion zones while decreasing the handled amount of radioactive sample. A plateau duration t_P of some tens of seconds is considered to be required to reach good precision and accuracy levels in ICP-MS measurements. In the experiment shown in Fig. 3B, the injected amount Q_i of 100 ng of each solute in a 75 μm i.d. × 116 cm L_S capillary, allows to obtain t_P values of a few seconds under the current intensity of 9 μA. First, it is clear that current intensity and capillary inner diameter must be reduced in order to increase t_P and decrease Q_i. Their values were thus fixed at 1 μA (which can be easily controlled by the used power supply) and 30 μm (which presents no risk of blocking), respectively. The interdependence between t_P, Q_i and L_S was then studied. Increasing sample amounts were injected in 30 μm i.d. capillaries of different lengths and, for each separation carried out at 1 μA, plateau durations were determined by Eq. (2). To facilitate experimental work and data treatment, these experiments were carried out with the mono-capillary configuration, for the sample mixture of 4 lanthanides (Nd, Sm, Eu and Gd) and by increasing injected solute concentration at constant injection volume (30 nL).

Fig. 4A shows the results obtained for Eu (which corresponds to the lowest resolution) at two separation lengths: L_S=103 cm and L_S=56.4 cm. This study was performed for non-coated silica capillaries (dashed lines) and PVA-coated silica capillaries (dark lines). For a given separation length, the plateau formation ($t_P \neq 0$) needs the injection of a certain sample amount $Q_{i,\ min}$. With increasing amount of injected solute beyond limit, plateau duration t_P increases as the band width t_B increases and the diffusion zone width ($3\sigma_1+3\sigma_2$) becomes more and more negligible. t_P reaches a maximal value $t_{P,max}$ for an optimal injected amount $Q_{i,max}$. This $Q_{i,max}$ value cannot be exceeded because, beyond this limit (symbolized by a star), the sample is not completely separated and a mixed zone of increasing width is formed. $Q_{i,max}$ and $t_{P,max}$ increase when separation length L_S is increased (i.e. separation volume is increased) and EOF is reduced (i.e. dispersion zone width is decreased). For example, the injection of 7.5 ng on a PVA-coated silica capillary of 56.4 cm separation length allows to obtain a plateau duration of 20 s. With a non-coated silica capillary, a t_P value of 20 sec implies a separation length of 103 cm and an injected solute amount of 10 ng.

In order to reduce the injected concentration (down to a value that can be reached with nuclear samples) keeping the injected amount constant , we investigated the use of coupled capillary configuration. Fig. 4 B compares the t_P versus Q_i curves obtained from a mono-capillary configuration (capillary inner diameter=30 μm, separation length=70 cm, injection volume=30 nL) and a coupled capillary configuration (separation capillary inner diameter=30 μm, separation length=70 cm, injection capillary=150 μm i.d. × 8 cm length, injection volume=1.4 μL). Whatever was the configuration used, all capillaries were coated with PVA and current intensity was equal to 1 μA. Separation work already began in injection capillary and, with coupled capillary configuration, separation volume is probably larger than in mono-capillary configuration. Consequently, in coupled capillary configuration, the separation capacity measured by $Q_{i,\ max}$ is slightly large, and at constant current intensity, the isotachophoretic velocity is low, which allows to obtain the same plateau duration with a low injected amount (t_P=20 s for injection of 5.5 ng in coupled capillaries configuration and 7.5 ng in mono-capillary configuration). In short, with the selected electrolyte system, the optimal separation conditions correspond to the use of the coupled capillary configuration with 30 μm i.d. × 70 cm length PVA-coated separation capillary under 1 μA current intensity: plateau duration of 10–30 s are obtained for an injected solute amount of 3–7 ng.

Fig. 5 shows the isotachophoregram obtained for the separation of the 13 lanthanide mixture under these conditions. Thirteen plateaus are observed with an average resolution of 0.78.

3.4. Hyphenation between ITP and ICP–MS

In this section, the double capillary system with a CD detector was hyphenated with an inductively coupled plasma quadrupole mass spectrometer (ITP/CD/ICP–QMS). The separation was focused on the four lanthanides (Nd, Sm, Eu, and Gd) because these elements are of great interest for neutronic code validation and also the most difficult to separate. For ICP–QMS detection four non-interfered isotopes (^{146}Nd, ^{149}Sm, ^{151}Eu, and ^{157}Gd) were sequentially measured with a dwell time of 50 ms. As can be seen in Fig. 7 the ICP–QMS data with a shape of four quasi-rectangular bands corresponding to the solutes of interest nicely fit with the CD signal corrected here for the time-lag. The CD signal also presents a step before Nd elution corresponding probably to an unknown impurity noted as X.

From the ICP–QMS data, two different plateaus are observed for Eu elution. The main part of the signal is well located between Sm and Gd bands, while a minor band (shaded area between 31 and 31.5 min in Fig. 6), corresponding to about 3% of the main Eu

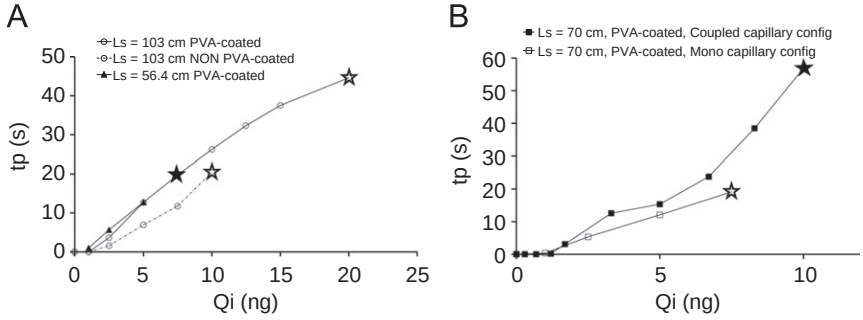

Fig. 4. Variations in plateau duration t_P versus injected Eu amount Qi for different conditions (see legends). Sample: 4 lanthanide mixture (Nd, Sm, Eu, and Gd). Leading electrolyte: 14 mM HMBA+10 mM acetic acid, pH value adjusted to 4.5 with ammonia. Terminating electrolyte: 15 mM acetic acid. Inner diameter of the separation capillary=30 μm. Current intensity=1 μA. (A) Separation length and (B) Injection volume.

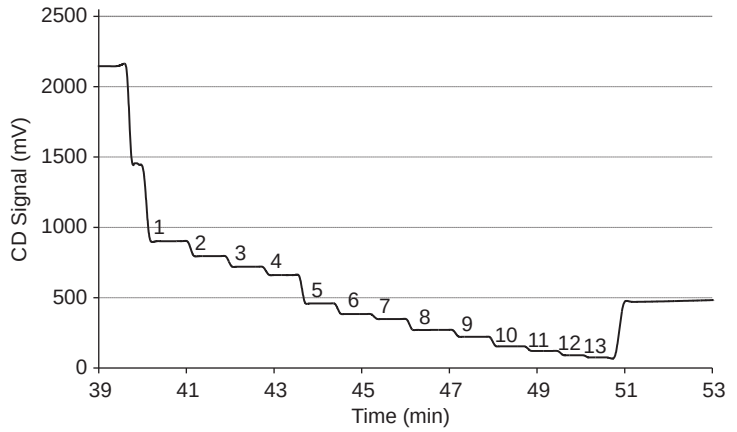

	Rs
(1)La	0.79
(2)Ce	0.78
(3)Pr	0.78
(4)Nd	0.80
(5)Sm	0.76
(6)Eu	0.79
(7)Gd	0.77
(8)Tb	0.83
(9)Dy	0.82
(10)Er	0.78
(11)Tm	0.72
(12)Yb	0.71
(13)Lu	0.76

Fig. 5. ITP–CD separation of lanthanides. Sample: 13 lanthanide mixture. Injected amount of each solute = 6.5 ng. Experimental conditions:coupled capillary configuration: 30 μm i.d. × 70 cm length PVA-coated separation capillary, 150 μm i.d. × 8 cm length PVA-coated injection capillary (injection volume = 1.4 μL). Leading electrolyte: 14 mM HMBA + 10 mM acetic acid, pH value adjusted to 4.5 with ammonia. Terminating electrolyte: 15 mM acetic acid. Current intensity = 1 μA.

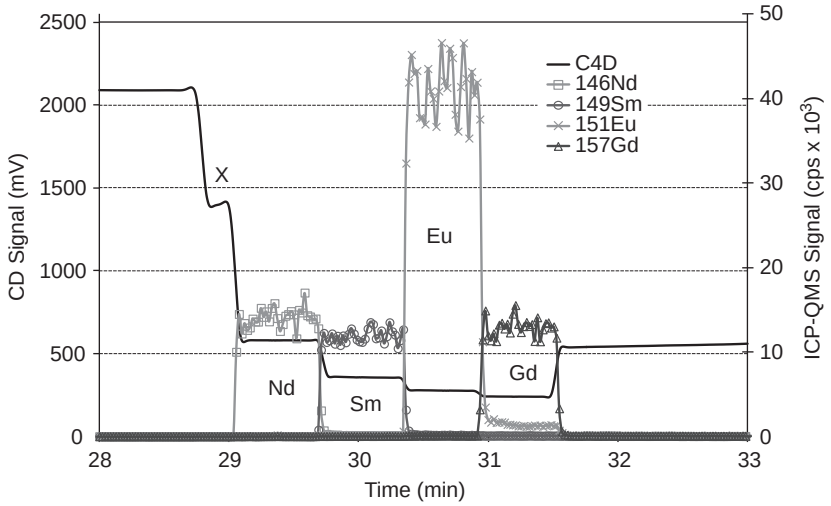

Fig. 6. ITP–CD–ICP–QMS separation of lanthanides (coincidence of CD and ICP–QMS signals is obtained by detector time-lag correction). Sample: 4 lanthanide mixture. Injected amount of each solute = 5 ng. X = impurity. Experimental conditions similar to Fig. 5.

band, is located within the Gd elution band. This minor signal is observed for both ^{151}Eu and ^{153}Eu isotopes whatever isotachophoretic and instrumental conditions. Thus the hypothesis of an isobaric interference at mass 151 is rejected. The presence in solution of two Eu subspecies like $EuOH^+$ and/or Eu(II) seems to be a more realistic scenario for explaining the two Eu plateaus. We should point out that the presence of $EuOH^+$ species in acid solution (pH ~ 4.5) seems rather unlikely because alkaline pH is necessary to form hydroxo-complexes of lanthanides [44]. In addition, this profile is not observed for the elution of Gd while hydroxo-complexe of Gd starts at lower pH than Eu. The stability of Eu(II) in solution is increased by the half-filled f subshell [45] unlike other elements. At lower oxidation number, acidity and electrophoretic mobility of Eu decrease. Consequently, the average electrophoretic mobility of Eu(II) complexed is getting close enough to Gd(III) complexed to migrate in the same band according to the ITP theory. Additional experiments may be conducted in order to identify the nature of the minor signal, however the ITP–ICP–QMS system remains able to solve the elution interference between isotopes of the minor Eu plateau and the Gd plateau.

A reconstituted sample MOx nuclear fuel has been analyzed by ITP–CD–ICP–QMS (Fig. 7). This sample contains a great number of elements (Table 1) able to be complexed with HMBA and to trouble ITP separation between the lanthanides of interest (Nd, Sm, Eu and Gd). The ICP–QMS signals (Fig. 7B) observed for the different isotopes demonstrate that the method allows having a complete inventory of the 4 lanthanides although the separation between the 24 elements present in the sample is not complete: indeed, there are only 8 solute plateaus visible on the CD signal (Fig. 7A). The ICP–QMS signals obtained for Gd isotopes are not rectangular bands but peaks because the injected amount (2.9 ng) of this element in this experiment is too low.

ITP–ICP–QMS experiments show that hyphenation of ITP with ICP–MS should be probably of great interest for isotope ratio measurements providing transient signals with a plateau. In addition, unlike IEC–ICP–MS or CE–ICP-MS, the R_s definition in ITP can be used in this new coupling to mathematically determine the signal portions suitable for isotope ratio measurements.

However, in this work, the sequential isotope measurements provided by the quadrupole spectrometer does not allow to obtain high isotope ratio precision and accuracy. For this task, a

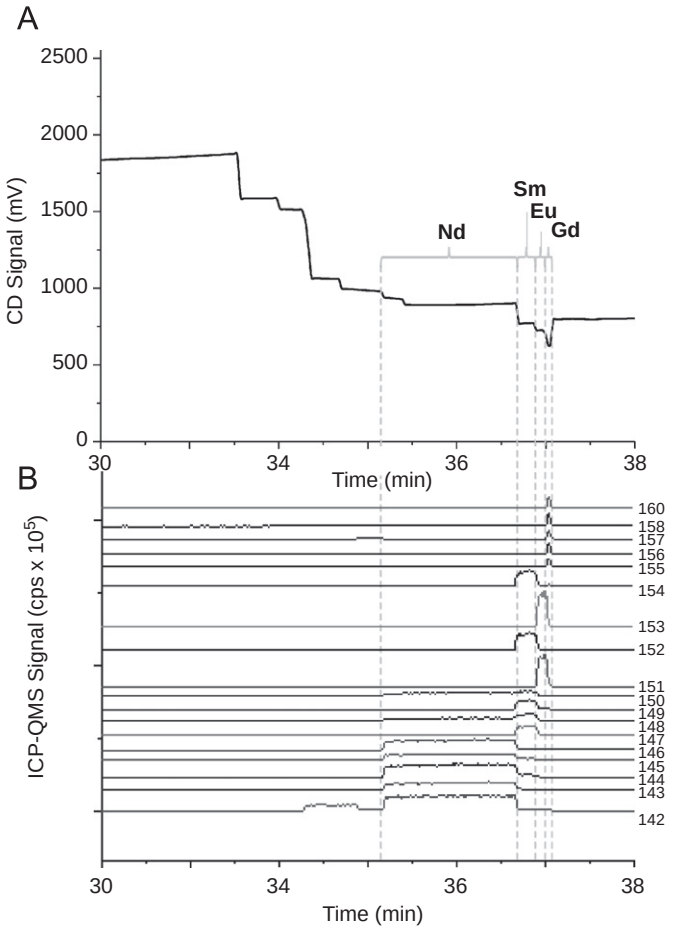

Fig. 7. ITP–CD–ICP–QMS separation of a simulated spent MOX fuel (coincidence of CD (A) and ICP–QMS (B) signals is obtained by detector time-lag correction). Injected concentration of each solute=see Table 1. Experimental conditions similar to Fig. 5.

multi-collection mass spectrometer is required. The accuracy using such a detector is about 0.5% [46].

4. Concluding remarks

This paper shows the application of a new electrolytic system for the mutual separations of almost all the individual members (13 out of 15) of the lanthanide series by isotachophoresis. This new system is based on a leading electrolyte that incorporates HMBA as complexing agent. This weak organic acid was proved to be 20% more selective than HIBA that is classically used for ITP separation of rare-earth elements. The optimization studies and technical developments allowed to propose a new methodology for lanthanide separation could be applicable on nuclear fuel samples. Furthermore we have demonstrated in this study that ITP separation could be directly coupled with ICP–MS and the quasi-steady state acquisition of ion beams should probably be of great interest for isotope ratio measurements. To date, the ITP system concentrate the sample injected 100 times which corresponds to a dose reduction by a factor 20, compared to a recent study with CE–ICP–QMS [14], without compromises on isotopic measurements performances. As the preconcentration factor depends only on the leading electrolyte composition and system geometry, the injection volume could be increased as much as the corresponding separation length is concerned. The hyphenation of ITP to ICP–MS thus allows minimizing handled sample amount, liquid waste volume and contacting time of the analyst with radioactive samples.

Acknowledgments

Dr. J.L. Rocca is deceased on 18 September 2009 and this article is dedicated to the great scientist he was. The co-authors are grateful to Dr. J.L. Rocca for his invaluable advices and his great interest for the development of micro total analysis systems.

References

[1] P. Leconte, JF. Vidal, D. Bernard, A. Santamarina, R. Eschbach, J.P. Hudelot, Ann. Nucl. Energy 36 (2009) 362.
[2] L.W. Green, C.H. Knight, T.H. Longhurst, R.M. Cassidy, Anal. Chem. 56 (1984) 696.
[3] F. Chartier, M. Aubert, M. Pilier, Fresenius. J. Anal. Chem. 364 (1999) 320.
[4] H. Isnard, R. Brennetot, C. Caussignac, N. Caussignac, F. Chartier, Int. J. Mass Spectrom. 246 (2005) 66.
[5] JJ. Bevelacqua, Health Phys. Soc. 98 (2010) S39.
[6] R. Brennetot, AL. Becquet, H. Isnard, C. Caussignac, D. Vailhen, F. Chartier, J. Anal. At. Spectrom. 20 (2005) 500.
[7] JG. Alonso, F. Sena, P. Arbore, M. Betti, L. Koch, J. Anal. At. Spectrom. 10 (1995) 381.
[8] JM. Barrero Moreno, JG. Alonso, P. Arbore, G. Nicolaou, L. Koch, J. Anal. At. Spectrom. 11 (1996) 929.
[9] M. Bourgeois, H. Isnard, A. Gourgiotis, G. Stadelmann, C. Gautier, S. Mialle, A. Nonell, F. Chartier, J. Anal. At. Spectrom. 26 (2011) 1549.
[10] W. Kerl, JS. Becker, W. Dannecker, HJ. Dietze, Fresenius. J. Anal. Chem. 362 (1998) 433.
[11] S. Röllin, Z. Kopajtic, B. Wernli, B. Magyar, J. Chromatogr. A 739 (1996) 139.
[12] I. Günther-Leopold, N. Kivel, J. Kobler Waldis, B. Wernli, Anal. Bioanal. Chem. 390 (2008) 503.
[13] C. Ambard, A. Delorme, N. Baglan, J. Aupiais, F. Pointurier, C. Madic, Radiochim. Acta 93 (2005) 665.
[14] A. Pitois, LA. Heras, M. Betti, Int. J. Mass Spectrom. 270 (2008) 118.
[15] JA. Day, JA. Caruso, JS. Becker, H. Dietze, J. Anal. At. Spectrom 15 (2000) 1343.
[16] T. Hirokawa, H. Okamoto, N. Ikuta, Electrophoresis 22 (2001) 3483.
[17] FM. Everaerts, M. Geurts, FEP. Mikkers, TPEM Verheggen, J. Chromatogr. A 119 (1976) 129.
[18] P. Janoš, Electrophoresis 24 (2003) 1982.
[19] DJ. Barkley, M. Blanchette, RM. Cassidy, S. Elchuk, Anal. Chem. 58 (1986) 2222.
[20] RM. Cassidy, S. Elchuk, NL. Elliot, LW Green, CH. Knight, BM. Recoskie, Anal. Chem. 58 (1986) 1181.
[21] P. Dufek, M. Vobecký, J. Holík, J. Valásek, J. Chromatogr. 435 (1988) 249.
[22] S. Elchuk, RM. Cassidy, Anal. Chem. 51 (1979) 1434.
[23] J. Hwang, JS. Shih, YC. Yeh, S. Wu, Analyst 106 (1981) 869–873.
[24] K. Cheng, Z. Zhao, R. Garrick, FR. Nordmeyer, ML. Lee, JD. Lamb, J. Chromatogr. A 706 (1995) 517.
[25] F. Foret, S. Fanali, A. Nardi, P. Bocek, Electrophoresis 11 (1990) 780.
[26] SP. Verma, R. García, E. Santoyo, A. Aparicio, J. Chromatogr. A 884 (2000) 317.
[27] YT. Yang, JW. Kang, JM. You, QY. Ou, Anal. Lett. 31 (1998) 1955.
[28] T. Hirokawa, W. Xia, Y. Kiso, J. Chromatogr. A 689 (1995) 149.
[29] Q. Mao, Y. Hashimoto, Y. Manabe, N. Ikuta, N. Fumitaka, T. Hirokawa, J. Chromatogr. A 802 (1998) 203.
[30] NM. Raut, PG. Jaison, SK. Aggarwal, J. Chromatogr. A 959 (2002) 163.
[31] P. Gebauer, P. Bocek, J. Chromatogr. 320 (1985) 49.
[32] FEP. Mikkers, EM. Everaerts, JAF. Peek, J. Chromatogr. A 168 (1979) 293.
[33] P. Gebauer, P. Bocek, Electrophoresis 16 (1995) 1999–2007.
[34] J. Petit, V. Geertsen, C. Beaucaire, M. Stambouli, J. Chromatogr. A 1216 (2009) 4113.
[35] C. Madic, M. Lecomte, P. Baron, B. Boullis, Comp. Phys. 3 (2002) 797.
[36] WP. Stagg, JE. Powell, Inorg. Chem. 3 (1964) 242.
[37] JE. Powell, AR. Chughtai, JW. Ingemanson, Inorg. Chem. 8 (1969) 2216.
[38] EN. Rizkalla, GR. Choppin, KA. Gscheidner, GH. Lander (Eds.), Handbook on the Physics and Chemistry of Rare Earths, Elsevier, 1994.
[39] P. Bocek, P. Gebauer, M. Deml, J. Chromatogr. 217 (1981) 209.
[40] M. Macka, P. Nesterenko, P. Andersson, PR. Haddad, J. Chromatogr. A 803 (1998) 279.
[41] T. Hirokawa, Y. Hashimoto, J. Chromatogr. A 772 (1997) 357.
[42] N. Kaltsoyannis, P. Scott (Eds.), The F Elements, Oxford Science Publications, 1999.
[43] L. Perna, F. Bocci, L. Aldave de las Heras, J. De Pablo, M. Betti, J. Anal. At. Spectrom. 17 (2002) 1166.
[44] CF. Baes, RE. Mesmer (Eds.), The Hydrolysisof Cations, John Wiley & Sons, New York, 1976.
[45] S Cotton (Ed.), Lanthanides and Actinides Chemistry, John Wiley & Sons, New York, 2006.
[46] L. Vio, G. Crétier, F. Chartier, V. Geertsen, A. Gourgiotis, H. Isnard, P. Morin, JL Rocca, J. Analyt. Atom. Spectrom. 27 (2012) 950.